

# Determination of Industrial Sulfur Dioxide Emissions and Mapping by Geographic Information System

Miray Başar Macit, Mahnaz Gümrükçüoğlu\*

Environmental Engineering Department, Sakarya University, Sakarya, Turkey

Received: 31 May 2011

Accepted: 12 October 2011

## Abstract

As the technology continuous to develop, air pollution has started to become more of a problem and it has started to threaten life in industrial regions. This study aims to calculate the sulfur dioxide (SO<sub>2</sub>) emission concentrations of industrial plants with the help of the Gauss Plume Model Equation, to map their distributions and, in regions where there is more than one industrial plant, to present the importance of total emissions. With this aim, in Sakarya city, three industrial plants that are close to each other and that use sulfur-containing fuels for energy were chosen, and the SO<sub>2</sub> emission concentrations coming out of their stacks were calculated in defined points of 50 m intervals. Total concentration values were determined and emission distribution is mapped using the geographic information system (GIS). As a result, although the emissions of the plants were below the standards, in the intersection regions of the emission plumes of the three plants it was seen that the total concentrations were at dangerous levels as far as air quality is concerned. In conclusion, it was found that it is important to calculate the emission distributions with air quality models and to show them with GIS to determine the pollution concentrations and distributions in advance. It is also important to evaluate the industrial plants on their own and compare them with other plants to inform the decision makers with the necessary information and to determine the necessary precautions.

**Keywords:** industrial air pollution, sulfur dioxide, Gauss Plume Model Equation, total emissions, geographic information system

## Introduction

The most common air pollutants are sulfur dioxide (SO<sub>2</sub>), carbon monoxide (CO), hydrocarbon, nitrogen oxide (NO<sub>x</sub>), ozone, and hydrogen sulfur (H<sub>2</sub>S). Of these elements, the main source of sulfur oxide (SO<sub>x</sub>) is industrial processes, fuels used for heating, and thermal power stations [1]. SO<sub>2</sub> constitute the most important amount in-between sulfur oxides that relate to the burning of fossil fuels [2]. Regions where industry is rapidly growing are

more likely to incur into industrial-based pollutants. A case in point is the Sakarya region in Turkey.

When studying air pollutants, it is imperative to model the pollution process. To combat air pollution problems in industrial and residential areas, air quality models can be used to evaluate and identify the necessary control levels [3]. A mathematical model expresses the diffusion and convection of a pollutant in the atmosphere and the models are applied separately for each pollutant. GIS plays a complementary role in the modeling and control of air pollution and supports the decision-making process.

In the literature there are various studies illustrating emission distributions related to air pollution and air quali-

---

\*e-mail: mahnaz@sakarya.edu.tr

ty control. They presented distribution of SO<sub>2</sub>, NO<sub>2</sub> or particulate matter from motor vehicles, domestic heating or industry by using modeling or GIS [4-16].

In this study, the sulfur dioxide emissions spreading out from three different industrial plants were examined, and Gauss Plume Model Equation concentration calculations were made to determine the total emission values and pollution distributions in the directions of dominant winds. By using this data, databases and thematic maps were created with GIS. The stacks of three different production plants were taken as the center of the study. We defined fields of size 1×1.5 km square for each plant in the dominant wind direction, (which was northwesterly) and we considered the intersection regions of emission plume of the plants as "Investigation Fields." The plants were named A, B, and C. The SO<sub>2</sub> concentrations of Plants B and C reached their highest values at a distance of 250 m after the stack exit; the highest concentration value for plant A was at a distance of 700 m. This situation was clearly seen in the thematic maps. The total concentration values in the intersection fields of the emission plumes were much higher than the values of any single plant. The joint effects of the plants was in fact one of the main goals of the study. For this reason, the emissions were also calculated in the intersection fields of the plume and thematic maps were created with separate databases. When the plants were examined one by one their emission values did not reach dangerous levels as in the intersection regions of the plumes. These results show the importance of measuring the joint effect concentrations in industrial zones.

## Material and Method

### Study Area

The study area, the city of Sakarya, is situated in north-west Turkey between 29-27 eastern meridians and 40-41 northern parallels (Fig. 1). The average height of the

province is only 31 m, which is a result of the fact that the major part of the province consists of plains and of low altitude hills. Plants we have collected in this study are on the borders of Akyazı district of Sakarya city [17].

Sakarya has a humid and temperate climate. Its average annual rainfall is 1025.8 mm. The relative humidity is about 72%. Winds generally blow from the north, northeast, and northwest. The average annual wind speed is 1.0 m/sec [17].

Data was collected from three industrial plants that use sulfur in the production process. In Plant A, which is south of the study field, paint-polishing and confection production is being carried out. Plant B, located north of the study field, processes jeans dyeing, and Plant C is home to cloth knitting and washing.

The emission data used in the calculation of SO<sub>2</sub> concentration values was taken from the 2006 Emission Measurement Reports of Sakarya City Environment and Forestry Head Office; the meteorological data was taken from the 2006 Environment Condition Report of Sakarya City Environment and Forestry Head Office.

### Concentration Calculations

The necessary data for the Gauss plume model equation used in the study is: wind speed and direction, atmospheric turbulence, medium air temperature, pollutant emission amount, source location and height, stack diameter, exit velocity, and exit temperature. The altitude of the study field was ignored in this study since it was negligible. Also, since there were no natural and artificial obstacles in the convection route of the spreading plume, the topography effects were ignored.

The Gauss plume model equation of the gas and aerosol for the central line ( $y=0$ ) of the emission plume is shown in the equation below for the concentration calculation Eq. (1).

$$C(x, 0, 0; H) = \frac{Q}{2\pi \sigma_y \sigma_z u} \exp\left[-\frac{1}{2}\left(\frac{H_{eff}}{\sigma_z}\right)^2\right] \quad (1)$$

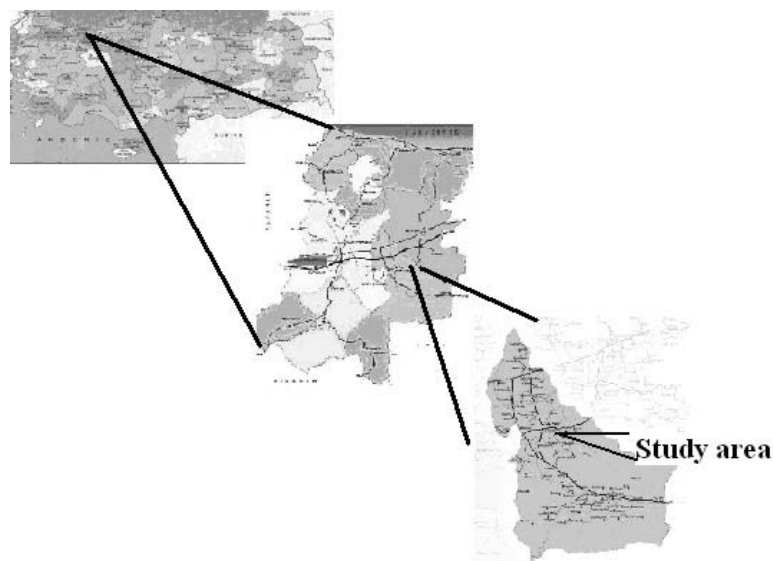


Fig. 1. Sakarya City and study area location map.

The equation used to calculate the concentration at earth level ( $z=0$ ) is shown in the equation below Eq. (2).

$$C(x, y, 0; H) = \frac{Q}{2\pi \sigma_y \sigma_z u} \exp\left[-\frac{1}{2}\left(\frac{y}{\sigma_y}\right)^2\right] \exp\left[-\frac{1}{2}\left(\frac{H_{eff}}{\sigma_z}\right)^2\right] \quad (2)$$

where:

- $C$  = Emission concentration, ( $g/m^3$ )
- $x$  = Emission source distance from a point on wind direction (m)
- $y$  = Distance two side from plume center line (m)
- $z$  = Distance from ground level to (m)
- $Q$  = Pollutant emission amount (g/sec)
- $u$  = Wind speed (m/s)
- $H$  = Stack height
- $H_{eff}$  = Effective stack height
- $\sigma_z$  = Vertical standard deviation (m)
- $\sigma_y$  = Horizontal standard deviation (m)

For calculating the standard deviation values of  $\sigma_y$  and  $\sigma_z$ , the necessary conditions were taken from Table 1 [18]. For equal distance, the centers of all three plants, the standard deviation values were equal. 30 numbers of  $\sigma_y$  and  $\sigma_z$  standard deviations were calculated for each plant.

The atmospheric stability classes were classified from A to F in 6 categories according to the Pasqual stability classes table, where A is very unstable, B is unstable, C is slightly unstable, D is neutral, E is slightly stable, and F is stable.

The higher the stack the more important the dispersion of the pollutants. When the stack is high, the plume sinks down to the ground only after a long distance and after the wind has ensured a better dispersion of the plume [19]. The effective stack height  $H_{eff}$  is the height at which the regular level of emission plume center line forms. This is obtained by adding the physical height of the stack and height of the emission plume. In the effective height calculations, emission and meteorological data were used and the effective stack heights were calculated separately for each plant.

Emission plume height is the difference between heights where the emission plume forms a regular level ( $H_{eff}$ ) and the physical stack height ( $H_s$ ). This height was calculated with the Holland (1953) equation using height,

wind speed, atmospheric pressure, medium temperature and gas temperature values [20].

The equation used in the calculations of the  $SO_2$  values is shown below Eq. (3).

$$C(x, y, 0; H) = C(x, 0, 0; H) \times \exp\left[-\frac{1}{2}\left(\frac{y}{\sigma_y}\right)^2\right] \quad (3)$$

- $C$  = Emission concentration, ( $g/m^3$ )
- $x$  = Emission source distance from a point on wind direction (m)
- $y$  = Distance two side from plume center line (m)
- $H$  = Stack height
- $\sigma_y$  = Horizontal standard deviation (m)

The data related to the investigated plants taken from the City Environment and Forestry Head Office is shown in Table 2.

Plant stacks were taken as center points and  $1 \times 1.5$  km square fields were identified as the investigation field for each plant, which was partitioned into  $50 \times 50$  m grids. In the analysis of the investigation fields, the dominant wind direction was taken into consideration. The whole area formed by the investigation fields of the three plants was evaluated as the "Study Field". In the investigation fields, by taking the stacks of each plant as the center, measurements were done in the fields where the emission plume formed in the dominant wind directions of each plant. 630 coordinate points were determined for each plant field, hence a total of 1890 points were marked in the satellite image of Sakarya, and their emissions values were calculated. The emission plume movement depends on the  $SO_2$  concentration of a plant and MapInfo Professional 8.5 SCP software was used to illustrate them. From the total  $SO_2$  concentration values of the intersection fields of the emission plume of the plants, the common effects of the plants were presented and they were mapped separately.

In the system considered here the origin is at ground level or beneath the point of emission, with the  $x$ -axis extending horizontally in the direction of the mean wind. The  $y$ -axis is in the horizontal plane perpendicular to the  $x$ -axis, and the  $z$ -axis extends vertically. The plume travels along or parallel to the  $x$ -axis [20]. The emission plume moved along or parallel to the  $x$ -axis. By taking the plant

Table 1. Coefficients for calculation of  $\sigma_y$  and  $\sigma_z$ .

Category of Stability	a	b	x<1 km			x>1 km		
			c	d	f	C	d	f
A	213	0.894	440.8	1.941	9.27	459.7	2.094	-9.6
B	156	0.894	106.6	1.149	3.3	108.2	1.098	2.0
C	104	0.894	61.6	0.911	0	61.0	0.911	0
D	68	0.894	33.2	0.725	-1.7	44.5	0.516	-13.0
E	50.5	0.894	22.8	0.678	-1.3	55.4	0.305	-34.0
F	34	0.894	14.35	0.740	-0.35	62.6	0.180	-48.6

Table 2. Data of plants.

	Plant A	Plant B	Plant C
Fuel type	Natural gas	Coal	Coal
Year of emission measurement	2006	2006	2006
Altitude of Stack	18 m	24.5 m	24 m
Flow of gas in measurement time (Q)	46956 m <sup>3</sup> /hour	11816.450 m <sup>3</sup> /hour	18753 m <sup>3</sup> /hour
Speed of gas (Vs.)	12.700 m/sn	8.5 m/sn	4.6 m/sn
Stack cross-section (d)	1.823 m	0.696 m	1.2 m
SO <sub>2</sub> emission	1.842 g/sn	1.608 g/sn	3.861 g/sn
Gas temperature (Ts)	501.15 K	329.950 K	324.150 K
Average annual wind speed (u)	1 m/sn	1 m/sn	1 m/sn
Environment air temperature (Ta)	297.55 K	297.55 K	297.55 K
Atmospheric Pressure	1012.9 mb	1012.9 mb	1012.9 mb

stacks as the centers, the lines on which SO<sub>2</sub> concentrations were calculated as the  $x$ -axis in the direction of the dominant winds were defined as the central lines. On the central line  $y=0$ .

Within the investigation region, in order to calculate the concentration values at 630 points that were designated at intervals of 50 m in the  $x$  and  $y$  directions for each plant, first the SO<sub>2</sub> concentrations had to be calculated on the central line. To this effect, the SO<sub>2</sub> concentrations were calculated at 30 points on the central lines of each plant. Thus, for any given plant, in 1.5 km along the  $x$ -axis and 500 m along  $\pm y$ -axes were sampled at 50 m intervals, using the Gauss distribution equation, and SO<sub>2</sub> concentrations were calculated. The set of calculation points in the investigation field was denoted as  $C(x, \pm y)$ . In this expression,  $C$  defines the concentration of SO<sub>2</sub>,  $x$  is the distance to the plant stack, and  $\pm y$  show the lateral distances in the positive and negative directions. Notice that the standard deviation values are considered identical in both cross-directions, and hence the calculated concentrations are the same. The calculation points of belonging to the intersection fields of the emission plume were separately determined and SO<sub>2</sub> values were calculated. We assumed in the calculations that the emissions within the investigation field were not subjected to any physical or chemical change.

The satellite image of Sakarya taken from the Google Earth software was used as a base map, on which the coordinates of the calculation points were determined. Using the world coordinates from this map, the concentrations at the corresponding points and their relative coordinates with respect to the plant center, a database was created for each plant. This resulted in a thematic map of the emission plume that pictured the SO<sub>2</sub> concentration distribution of each plant. The lowest and the highest concentration values of each plant were marked with 15 different colors. Concentrations below 1 µg/m<sup>3</sup> were neglected. Since the plants' locations were close to each other, the SO<sub>2</sub> emission

plume in the dominant wind directions of the plants overlaps and forms an intersection field in some regions. The coordinates of the sampling points in the overlapping regions were designated independently from the investigation fields of the plants, and the total SO<sub>2</sub> concentrations were calculated. In all of the created thematic maps, the SO<sub>2</sub> concentration values of the facilities were shown in colors in a range such that the highest concentration was represented with red and the lowest concentration with light blue.

## Results

The SO<sub>2</sub> concentration values of the three plants at the points were calculated. Fig. 2 demonstrates the concentration calculation points of the three plants.

The standard deviation values calculated depending on the distances from the plant centers along the dominant wind direction are shown in Table 3.

Emission plume height and effective stack height of plants have been calculated and shown in Table 4.

SO<sub>2</sub> concentration values for calculation points are shown in graphs. Fig. 3 demonstrates the graph of Plant C.

In an area of size 1×1.5 km where the stack of Plant C is considered as the center, the maximum SO<sub>2</sub> concentration value was calculated as 212.332. As shown in Fig. 3, the SO<sub>2</sub> concentration of Plant C along the central line was 20 µg/m<sup>3</sup> at a distance of 100 m, but at 250 m it reached to 212.232 µg/m<sup>3</sup>, which is also the maximum value, and decreased thereafter rapidly. Due to the ideal shape of the emission coming out of the stack [21], the concentration value on the  $y$ -axis makes a peak at a distance larger than 250 m. For instance, the peak at  $y=50$  m from the central axis occurs at  $x=300$  m, and the peak point  $y=150$  m occurs at  $x=650$  m. More specifically, the SO<sub>2</sub> concentration at point C(300, ±50) is 128.927 µg/m<sup>3</sup>, and at point C(450, ±100) it is 56.321 µg/m<sup>3</sup>. Fig. 4 shows the SO<sub>2</sub> emission

Table 3. Standard deviation values.

x (m)	$\sigma_y$	$\sigma_z$	x (m)	$\sigma_y$	$\sigma_z$
50	10,715	6,711	800	127,787	85,791
100	19,912	10,864	850	134,904	91,742
150	28,612	15,353	900	141,977	97,746
200	37,004	20,074	950	149,008	103,799
250	45,173	24,977	1000	156	109,9
300	53,171	30,028	1050	162,955	116,692
350	61,027	35,207	1100	169,875	119,938
400	68,765	40,498	1150	176,762	128,146
450	76,401	45,889	1200	183,617	134,181
500	83,947	51,37	1250	190,442	140,24
550	91,413	56,933	1300	197,238	146,324
600	98,808	62,572	1350	204,006	152,43
650	106,138	68,282	1400	210,748	158,558
700	113,408	74,058	1450	217,464	164,708
750	120,623	79,895	1500	224,156	170,879

plume distribution of Plant C. SO<sub>2</sub> emission concentration increases rapidly after stack exit and decreases slowly thereafter as seen in this emission distribution map. The regions with highest emissions are in black. The emission plume colors are getting to light gray when the concentration decrease and different tones of gray color present less concentration.

Along the central line of Plant B the SO<sub>2</sub> concentration is 7.035 µg/m<sup>3</sup> at 100 m and reaches its maximum value of

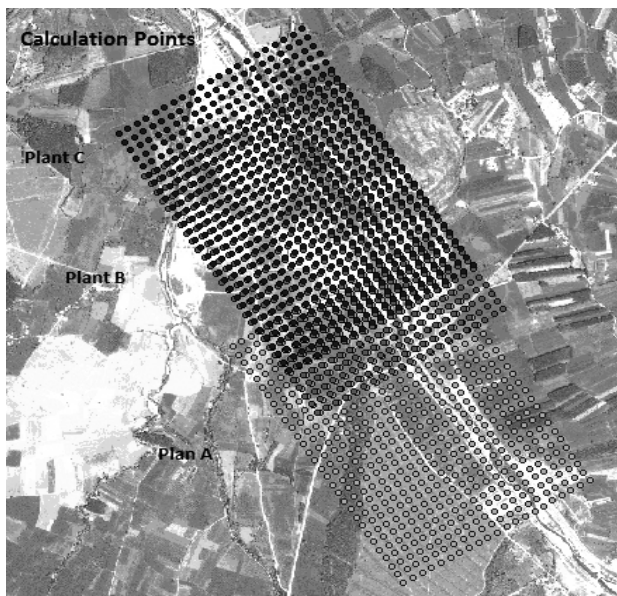


Fig. 2. Concentration calculation points for three plants.

Table 4. Emission plume heights and effective stack heights of plants.

	Plant C	Plant B	Plant A
Emission Plume Height (m)	10.292	10.283	83.439
Effective Stack Height (m)	34.292	34.783	101.439

86.042 µg/m<sup>3</sup> at 250 m. Fig. 5 demonstrates the SO<sub>2</sub> concentration value of Plant B peaking at 250 m, with a behavior similar to that of Plant C. Other SO<sub>2</sub> concentration estimates read as follows: C(300, ±50) = 52.684 µg/m<sup>3</sup>, and C(450, ±100) = 23.26 µg/m<sup>3</sup>. Samples of the peak concentrations on the y-axis are at C(100, ±450) and C(200, ±900) pointing to the spreading of the plume.

Fig. 6 demonstrates that the situation is clearly seen in the thematic maps. SO<sub>2</sub> emission concentrations increase rapidly after stack exit in the thematic map. The region of more than 63 µg/m<sup>3</sup> of SO<sub>2</sub> emission concentration is presented as a black color. The lower concentration values are shown in different tones of gray.

In Fig. 7 it is seen that for Plant A, the concentration value of SO<sub>2</sub> peak at 700 m on the x-axis (different from the other plants), and then starts to fall down afterwards. Along the central line the SO<sub>2</sub> concentration is 0.068 µg/m<sup>3</sup> at 250 m, and rises to 9.768 µg/m<sup>3</sup> at 500 m. It reaches to 13.66 µg/m<sup>3</sup> at 700 m, which is the highest value. After the 700th m, the concentration value starts to fall. However, the decrease rate of concentration is slower than that of the other two plants. For example, the concentration values at Plant C and Plant B decrease by 50% 300 m after the peak point, but this decrease is about 15% for Plant A. Due to the ideal shape of the emission distribution [21] having gone further away from the center in the y direction, the concentration value peaks at more than 700 m away from the stack in the x-axis. For instance, at 100 m away from the center in the axis, the peak point occurs at 800 m in the x-axis, but at 200 m away it occurs at 1100 m. Along the y-axis, for example at point C (700, ±50), the SO<sub>2</sub> concentration value is 12.472 µg/m<sup>3</sup>, and at point C (800, ±100) it reaches 9.789 µg/m<sup>3</sup>.

Fig. 8 demonstrates the concentration distribution map of Plant A. The SO<sub>2</sub> emission plume where the region of more than 12 µg/m<sup>3</sup> concentration value is presented as dark red color.

The SO<sub>2</sub> emission plume of the plants overlay in some regions and create intersection regions. In the regions shown in Fig. 9, the total SO<sub>2</sub> emission concentrations were calculated and maps were created by using the databases that were prepared for each region. In order to emphasize the common effects of the plants along the common wind region, which is the main purpose of this study, the SO<sub>2</sub> concentration distribution maps of the three plants are shown together in Fig. 9. According to Fig. 9, the region that overlays three plants emission plumes, especially in intersection regions, SO<sub>2</sub> emission reaches the highest value and this intersection region of plumes is clearly the most polluted region.

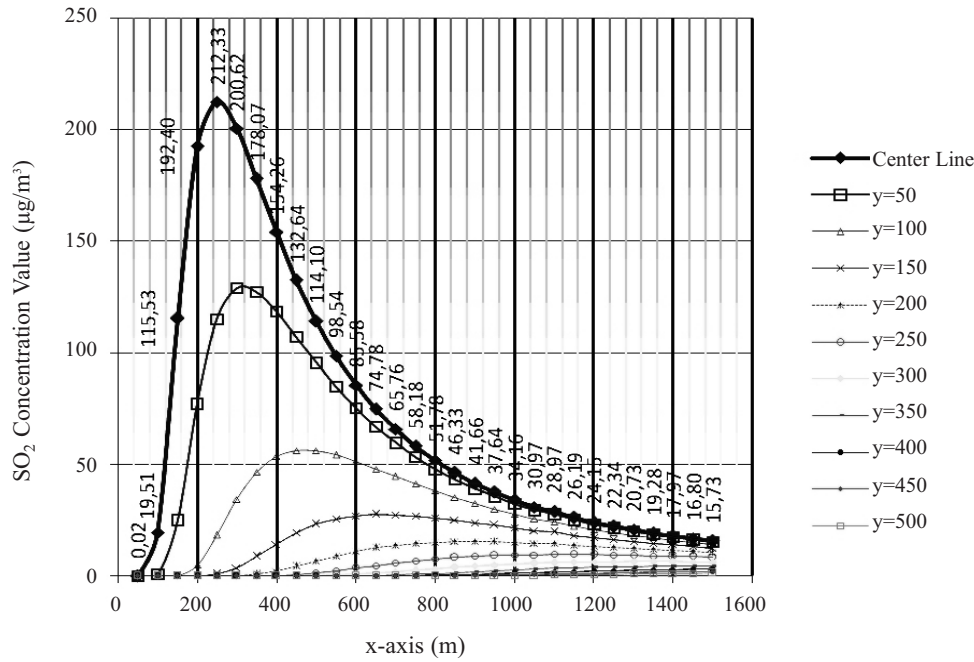


Fig. 3. SO<sub>2</sub> concentration values for plant C.

Fig. 10 demonstrates the intersection region maps of Plant C and Plant B emission plumes. Here, the highest SO<sub>2</sub> concentration value is 209.458 µg/m<sup>3</sup>, and the lowest concentration value is 1.259×10<sup>-17</sup> µg/m<sup>3</sup>.

Fig. 11 demonstrates the intersection region maps of Plant B and Plant A emission plumes. Here, the highest SO<sub>2</sub> concentration value is 18.069 µg/m<sup>3</sup> and the lowest concentration value is 0.0834 µg/m<sup>3</sup>.

Fig. 12 demonstrates the SO<sub>2</sub> concentration distribution shown for the field where the emission plume of the three plants intersect. In this intersection for the region of the emission plume of Plant C, B, and A, the highest SO<sub>2</sub> con-

centration value is 36.545 µg/m<sup>3</sup>, and the lowest concentration value is 0.795 µg/m<sup>3</sup>.

Taking the stack of Plant B as the center, in the center line, the SO<sub>2</sub> concentration value at 50 m is 0.00522 µg/m<sup>3</sup>, but since at the same point the SO<sub>2</sub> concentration value of Plant C is 200.61645 µg/m<sup>3</sup> the total concentration value at this point becomes 200.62167 µg/m<sup>3</sup>. The SO<sub>2</sub> concentration value of Plant C, which starts to reduce at 450 m, is 132.64424 µg/m<sup>3</sup>, but the SO<sub>2</sub> concentration of Plant B, which has a concentration value of 76.8133 µg/m<sup>3</sup> at 200 m on the center line, starts to increase at the same point and because of this the total concentration value reaches 209.45754 µg/m<sup>3</sup> at this point. The SO<sub>2</sub> concentration value of Plant C becomes 105.38870 µg/m<sup>3</sup> at 750 m on the centerline.

The SO<sub>2</sub> concentration value of Plant A in the center line at 50 m is 9.94298×10<sup>-47</sup> µg/m<sup>3</sup>, but since at the same point the SO<sub>2</sub> concentration value of Plant B is 14.20316 µg/m<sup>3</sup> the total concentration value at this point becomes 14.20316 µg/m<sup>3</sup>. With the concentration value of Plant B at this point, this point was colored in the map with the color that corresponds to 14.20316 µg/m<sup>3</sup> in the legend. The concentration value of Plant A in the center line at 550 m is 11.5223 µg/m<sup>3</sup>, whereas the concentration value of Plant B at the same point is 6.5467 µg/m<sup>3</sup>. The total concentration value at this point reaches 18.0690 µg/m<sup>3</sup>, which is higher than the highest SO<sub>2</sub> concentration value of Plant A.

**Discussion**

In between the three plants where SO<sub>2</sub> concentrations were calculated, the highest concentrations were observed on the center lines along the dominant wind directions, the



Fig. 4. SO<sub>2</sub> concentration distribution map for Plant C.

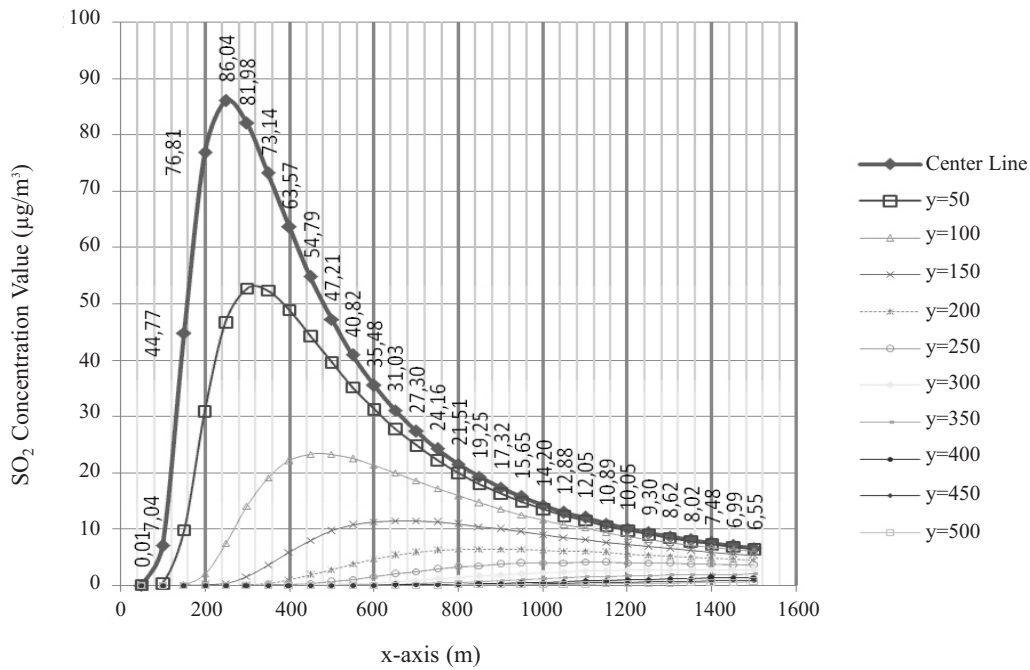


Fig. 5. SO<sub>2</sub> concentration values for Plant B.

plant stacks being the centers. As can be seen from the maps and graphs related to Plant C and B, the SO<sub>2</sub> concentrations are similar. Both plants have the highest SO<sub>2</sub> concentration values at 250 metres on the center line, and this coincidence is due to their similar effective stack heights. The effective stack heights of plants C and B show that the emission plumes reach a smooth level 10 meters after the stack. In Plant A, the situation is different from the others and the highest SO<sub>2</sub> concentration occurs at 700 meters on the center line. The emission cloud height of Plant A reaches a smooth value after 83.4 meters. The stack gas temperature and the stack exit velocities of Plant A are very dif-

ferent from the other two plants, and this causes a difference between the effective stack heights.

The total SO<sub>2</sub> concentrations in the intersection region of plants C and B can reach more than the SO<sub>2</sub> concentrations that the plants have on their own. At the points where the SO<sub>2</sub> concentration values of Plant C start to decrease, the concentration value of Plant B reaches its maximum value. For this reason, in the calculation points, although the SO<sub>2</sub> concentrations should be low due to a single plant, the SO<sub>2</sub> concentrations of another plant increase the total concentration in that field.

The intersection region of the three plants is at the final stage of the plumes of plants C and B, and therefore the SO<sub>2</sub> concentrations in this region, are lower than the worst case. Although the SO<sub>2</sub> concentration values of Plant A start to increase in this region, its concentrations are lower as compared to the other two plants, B and C, since Plant A uses natural gas. Although in the intersection region of the three plumes and along the direction of dominant wind, the SO<sub>2</sub> concentrations are low, but they are still approximately 3 times the SO<sub>2</sub> value if Plant A were the only factor in this region. Therefore, the total concentrations in the intersection regions of the emission plumes can potentially be significantly greater than those of individual plants. It is important to know the emissions of all the plants in the region to assess their common effect on air quality.

Related literature often cites emissions of individual plants without studying their cumulative effect. Joint study of pollution effects and investigation of various scenarios are necessary to determine the total pollution load of the region, to choose the correct location of new plants, and for assessing social costs.

Geographical Information Systems is a convenient tool for processing, analyzing, and presenting spatial data.

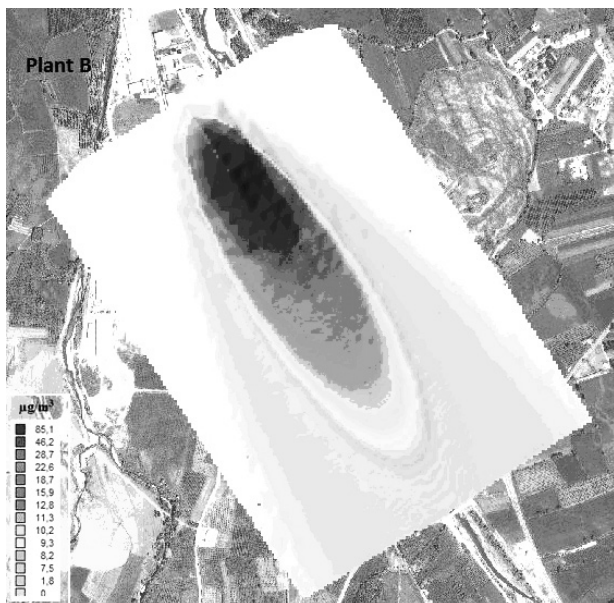


Fig. 6. SO<sub>2</sub> concentration distribution map for Plant B.

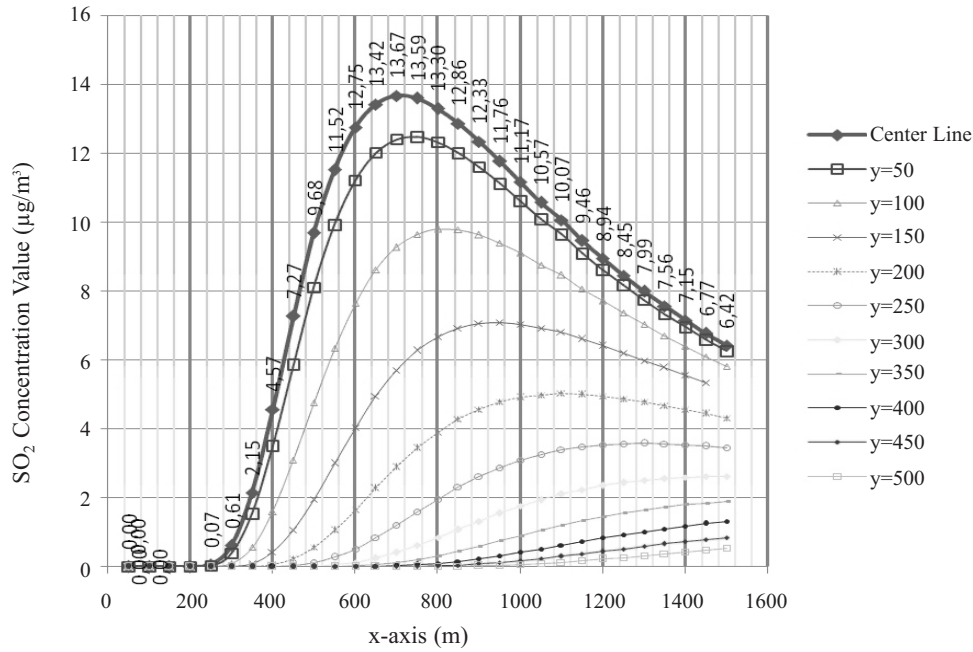


Fig. 7. SO<sub>2</sub> concentration values for Plant A.



Fig. 8. SO<sub>2</sub> concentration distribution map for Plant A.

Thematic maps created with GIS are indispensable in that they illustrate the spread of air pollutants, and they serve in planning and decision support systems.

**Conclusions**

Uncontrolled and unplanned industrialization invariably leads to deterioration of the environment and to air pollution. Air pollution dispersion models are highly specialized tools that usually have specifications in areas of applications [22]. With modeling, monitoring, and planning, many of the deleterious consequences can be avoided so that wealth-producing industry and an unpolluted environment can coexist.

In this case study, we considered a heavily industrialized area, investigated the SO<sub>2</sub> pollution due to three adjacent by plants in view of the dominant wind direction, the plume behavior with particular attention to the overlapping areas, and thematic maps were created.

Industry is developing rapidly in Sakarya city. For this reason, monitoring of industrial air pollution calculations of total concentrations are important. From this study, we can draw the conclusion that each industrial plant played important roles for total emissions in some areas. This study

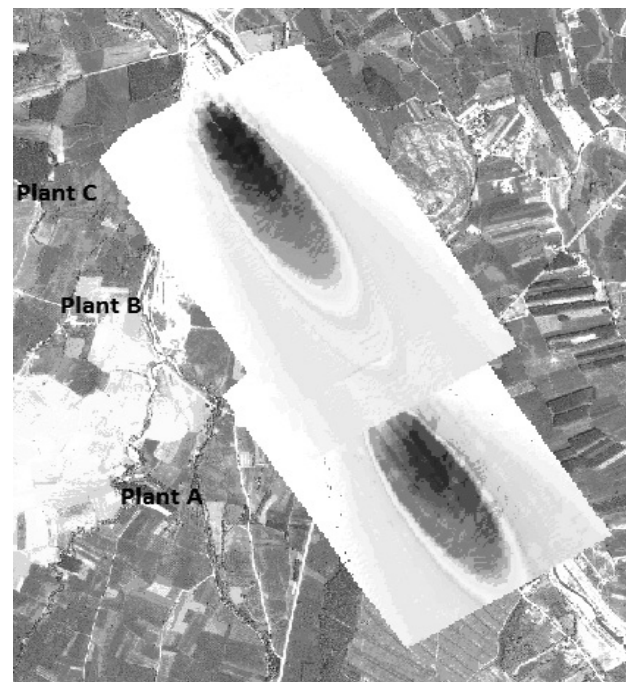


Fig. 9. SO<sub>2</sub> concentration distribution overlay map for plants C, B, and A.



Fig. 10. SO<sub>2</sub> concentration distribution map of emission plume intersection areas for plants C and B.

can be used as a basis for air pollution that originated from industry for Sakarya and highlights the way to the local administrators in the management of air quality of the city. Licensing a new plant requires the common effect of all the plants. It is also the first study about industrial pollution for Sakarya. Moreover, by using GIS, industrial emission concentration distributions can be shown, analyzed and updated, and future solutions of these problems can be suitable. So, calculated pollutant distributions and their illustrations on GIS-aided maps provide invaluable information for decision makers and planners.

According to the obtained results of this study, it is an absolute necessity to take precautions for reducing emissions. To reduce industrial emission fossil fuel usage should be minimized in industry. New technology and practice



Fig. 11. SO<sub>2</sub> concentration distribution map of intersection area for plants B and A.



Fig. 12. SO<sub>2</sub> concentration distribution map of intersection areas for plants C, B, and A.

should be built up for increasing burning units performance. In order to eliminate pollution, clean energy such as natural gas or geothermal energy should be generalized and evaluated. In areas where the highest pollution is detected, emission control techniques should be practiced and monitored. Emission standards should be determined according to total emission for each area. Emission measurements should be made regular by official institutions.

## References

1. AYDIN M., DURDURAN S., OZCAN S., BEDUK F. Evaluation of Air Quality Variation in Konya City by Using Geographic Information System, 7<sup>th</sup> National Environmental Engineering Congress, Izmir, Turkey. Available from: <http://e-kutuphane.cmo.org.tr/pdf/562.pdf>, 2007.
2. TUNAY O., ALP K. Air Pollution and Control, Chamber of Environmental Engineers Publishing, Istanbul Chamber of Commerce, Istanbul, 1996.
3. INCECIK S. Air Pollution, Istanbul Technical University Publishing, Istanbul, pp.72-76, 1994.
4. FERREIRA F., TENTE H., TORRES P., CARDOSO S., PALMA-OLIVEIRA J.M. Air Quality Monitoring and Management in Lisbon, Environ. Monit. Assess., 65 (1-2), 443, 2000.
5. TANRISEVER M. Modeling of Air Pollutants Distribution, Dissertation, Gazi University Publishing, Turkey, 1991.
6. RAGLAND K. Worst-Case Ambient Air Concentrations From Point Sources Using The Gaussian Plume Model, Atmos. Environ., 10, (5), 371, 1975.
7. LIN M., LIN Y. The Application of GIS To Air Quality Analysis in Taichung City, Taiwan, Environmental Modeling & Software, 17, (1), 11, 2002.
8. SENGUPTA S., PATIL R.S., VENKATACHALAM P. Assessment of population exposure and risk zone due to air pollution using the geographic information system, Comput. Environment and Urban Systems, 3, (20), 191, 1996.
9. FIALA J., REIDER M., DUARAKOVA M., LVOROVA H. Trends in the Atmospheric and Hydrological Cycle of Sulphur at Catchments in the Czech Republic, Atmos. Environ., 1, (35), 2001.

10. ELBİR T. A GIS based decision support system for estimation, visualization and analysis of air pollution for large Turkish cities, *Atmos. Environ.*, **38**, 4509, **2004**.
11. GUMRUKCUOGLU M. Urban Air Pollution Monitoring by Using Geographic Information Systems: A Case Study from Sakarya, Turkey, *Carpathian Journal of Earth and Environmental Sciences*, **6**, (2), 72, **2011**.
12. BALAKRISHNA G., PERVEZ S. Source Apportionment of Atmospheric Dust Fallout in an Urban-Industrial Environment in India, *Aerosol and Air Quality Research*, **9**, (3), 359, **2009**.
13. LIN C., WU Y., LAI C., WATSON J., CHOW J. Air Quality Measurements from the Southern Particulate Matter Supersite in Taiwan, *Aerosol and Air Quality Research*, **8**, (3), 233, **2008**.
14. HUNG I-F., DESHPANDE C.G., TSAI C-J., HUANG S.H. Spatial and Temporal Distribution of Volatile Organic Compounds around an Industrial Park of Taiwan, *Aerosol and Air Quality Research*, **5**, (2), 141, **2005**.
15. OWEN B., EDMUNDS H.A., CARRUTHERS D.J., RAPER D.W. Use of a New Generation Urban Scale Dispersion Model to Estimate the Concentration of Oxides of Nitrogen and Sulphur dioxide in a Large Urban Area, *Sci. Total Environ.*, **235**, (1-3), 277, **1999**.
16. UKPEBOR E.E., UKPEBOR J.E., EROMOMENE F., ODIASE J.I., OKORO D. Spatial and Diurnal Variations of Carbon Monoxide Pollution from Motor Vehicles in an Urban Centre, *Pol. J. Environ. Stud.*, **19**, (4), 817, **2010**.
17. CITY ENVIRONMENTAL REPORT. Sakarya Governorship, City Environment and Forestry Head Office. **2006**.
18. COOPER C.D., ALLEY F.C. Air Pollution Control, Waveland Publishing Inc., ABD, **1996**.
19. ALKAMA R., ADJABI S., AIT IDIR F., SLIMANI Z. Air Pollution in Bejaia City (Algeria): Measurements and Forecasts, *Pol. J. Environ. Stud.*, **19**, (5), 769, **2009**.
20. TURNER B. Workbook of Atmospheric Dispersion Estimates, Environmental Protection Agency, Office of Air Programs, Research Triangle Park, North Carolina, **1970**.
21. WEBER A.H. Atmospheric Dispersion Parameters in Gaussian Plume Modeling, Part I, Review Of Current Systems and Possible Future Developments, Epa-600/4-76-030a. **1976**.
22. FAGBEJA M. Applying Remote Sensing and GIS Techniques to Air Quality and Carbon Management- a Case Study of Gas-Flaring in the Niger Delta, Progression Report-Part 1, University of West of England, Bristol, **2008**.